CROP PROJECT: Deep Seismic Exploration of the Central Mediterranean and Italy
Edited by I.R. Finetti

CHAPTER 24

Seismic Modelling Applied to CROP Crustal Section in the Adriatic Sea

J.M. Carcione[1,*], I.R. Finetti[2], D. Gei[1]

ABSTRACT

We use a seismic-modelling methodology to validate the interpretation of a deep-crust seismic survey. We compute a zero-offset stacked section, with a single simulation, by using the exploding-reflector concept and the non-reflecting wave equation. The geological model is verified by computing exploding-reflector experiments and comparing them with the real stacked section. In the final phase of the modelling study, we use the variable-density acoustic wave equation to compute common-shot and common-offset synthetic surveys, which are used to obtain the synthetic stacked time section using the standard processing sequence. These simulations and verification of the geological model by post-stacked migration constitute an additional test. The methodology is applied to a seismic line from the Italian deep-crust exploration project CROP, acquired in the Adriatic Sea.

Keywords: seismic modelling, CROP, crustal section, Adriatic

1. INTRODUCTION

Seismic numerical modelling is a valuable tool for validation of seismic interpretations. The method has been used in hydrocarbon exploration (Fagin, 1992), earthquake-seismology (Priolo, 1999) and crustal studies (Yarnold et al., 1993; Morgante et al., 1998). Here, we develop a methodology for investigating the seismic response of the Earth's crust at the large-scale, with the purpose of interpreting the main geological features from the surface to the upper mantle.

The main deep-crust exploration project in Italy is CROP (Finetti, 1994; Finetti et al., 2001). It is the equivalent of DEKORP (Germany) (Rabbel and Gajewski, 1999), COCORP (USA), BIRPS (UK) and ECORS (France). The data was acquired on land and offshore in the Adriatic and throughout the central Mediterranean. In particular, the CROP M-15 seismic section was acquired offshore in the Adriatic Sea. The source and acquisition parameters for this deep seismic section are given in Table 1. Land CROP data obtained nearby in the Southern Apennines are exhibited in the literature (Mazzotti et al., 2000). Amplitude information is relatively important, but a precise determination of the interval velocities is difficult because the residual NMO of reflection events beyond 4–5 s becomes critically small. This fact precludes the use of accurate velocity analyses, reflection tomography, and techniques such as prestack depth migration. Therefore, we deal with almost zero offset P-wave data, and the model design is based on the interpretation of the stacked time section, since well data are scarce, and only oil exploration wells down to 4 km depth are available. We do not consider mode conversion (i.e., S waves) and intrinsic attenuation, which, in this situation, constitute second order effects. Anisotropy of the P wave is modelled with an elliptical anisotropic rheology, since it can be important in the upper mantle (Guest and Thomson, 1992).

The modelling method is based on the 2-D acoustic wave equation with variable density. This choice allows us to define the acoustic impedance of each macro-layer. The velocity field and density of each stratum can be defined on the basis of the reflector strength and global geological information for the study area. The data in the Adriatic Sea has a good signal-to-noise ratio, unlike onshore data, where strong tectonism in the Apennines region has created highly discontinuous reflectors. However, the signal is degraded by the heterogeneous nature of the crust

[1]Istituto Nazionale di Oceanografia e di Geofisica Sperimentale (OGS), Borgo Grotta Gigante 42c, 34010 Sgonico, Trieste, Italy
[2]EGG (Exploration Geophysics Group), Department of Geological, Environmental and Marine Sciences, Faculty of Sciences, University of Trieste, via Weiss 1, 34127 Trieste, Italy
*Corresponding author. Fax: +39 040 327521; e-mail: jcarcione@ogs.trieste.it (J.M. Carcione)

Table 1
Seismic vessel and acquisition parameters of CROP M-15 seismic survey

Seismic vessel	OGS-Explora
Source	Air-guns (80.4 l)
Recording length	17 s
Sampling interval	4 ms
Streamer length	4500 m
Group spacing	25 m
Shot interval	50 m
Channels	180
Coverage	4500%

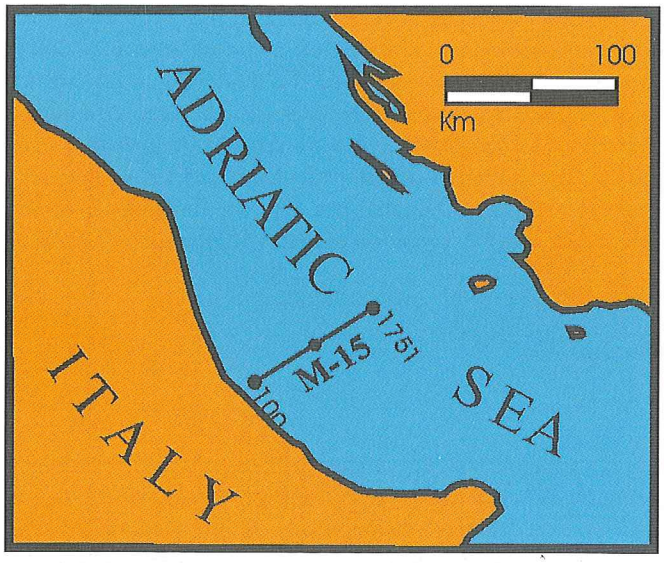

Figure 1: Location of the CROP M-15 seismic line in the Adriatic Sea.

at small scales. Constraints on the velocity variations of these small-scale heterogeneities can be estimated from P-wave sonic logs. We introduce these inhomogeneities by using a spatially isotropic von Kármán autocovariance probability function of high fractal dimension, which simulates scattering-Q effects (Holliger, 1997). A typical correlation length is 100 m and the standard deviation of the velocity fluctuations ranges from 200 to 400 m/s.

As the first step, a ray-tracing algorithm is used to obtain a preliminary geological model by comparing the synthetic (zero-offset) two-way travel times to those of the real stacked section. Simulation of a stacked seismic section requires the calculation of a set of common-shot experiments and application of the standard processing sequence. An approximation of the stacked section is obtained with the non-reflecting wave equation and the exploding-reflector approach. These methods allow us to reduce computing time (Baysal et al., 1984; Carcione et al., 1994). The non-reflecting wave equation implies a constant impedance model to avoid multiple reflections, which are, in principle, absent from stacked sections and constitute unwanted artifacts in migration processes. In the exploding-reflector method, each reflection point in the subsurface explodes at $t = 0$ with a magnitude proportional to the normal-incidence reflection coefficient. The non-reflecting equation is a modification of the wave equation, where the impedance is constant over the whole model space. In this way, non-physical multiple reflections are avoided and the recorded events are primary reflections. The density is used as a free parameter to obtain a constant impedance model and avoid multiple reflections. The reflection strength is then implicit in the source strength. Moreover, the method generates normal-incidence reflections, i.e., those having identical downgoing and upgoing wave paths. In order to obtain the two-way travel time, the phase velocities are halved. Due to sampling constraints, halving the velocities implies doubling the number of grid points. After a set of exploding-reflector experiments and comparison with the real stacked section, we obtain the final geological model. We do not consider anisotropy and scattering in this process. The "exact" synthetic stacked section is then obtained by applying the standard

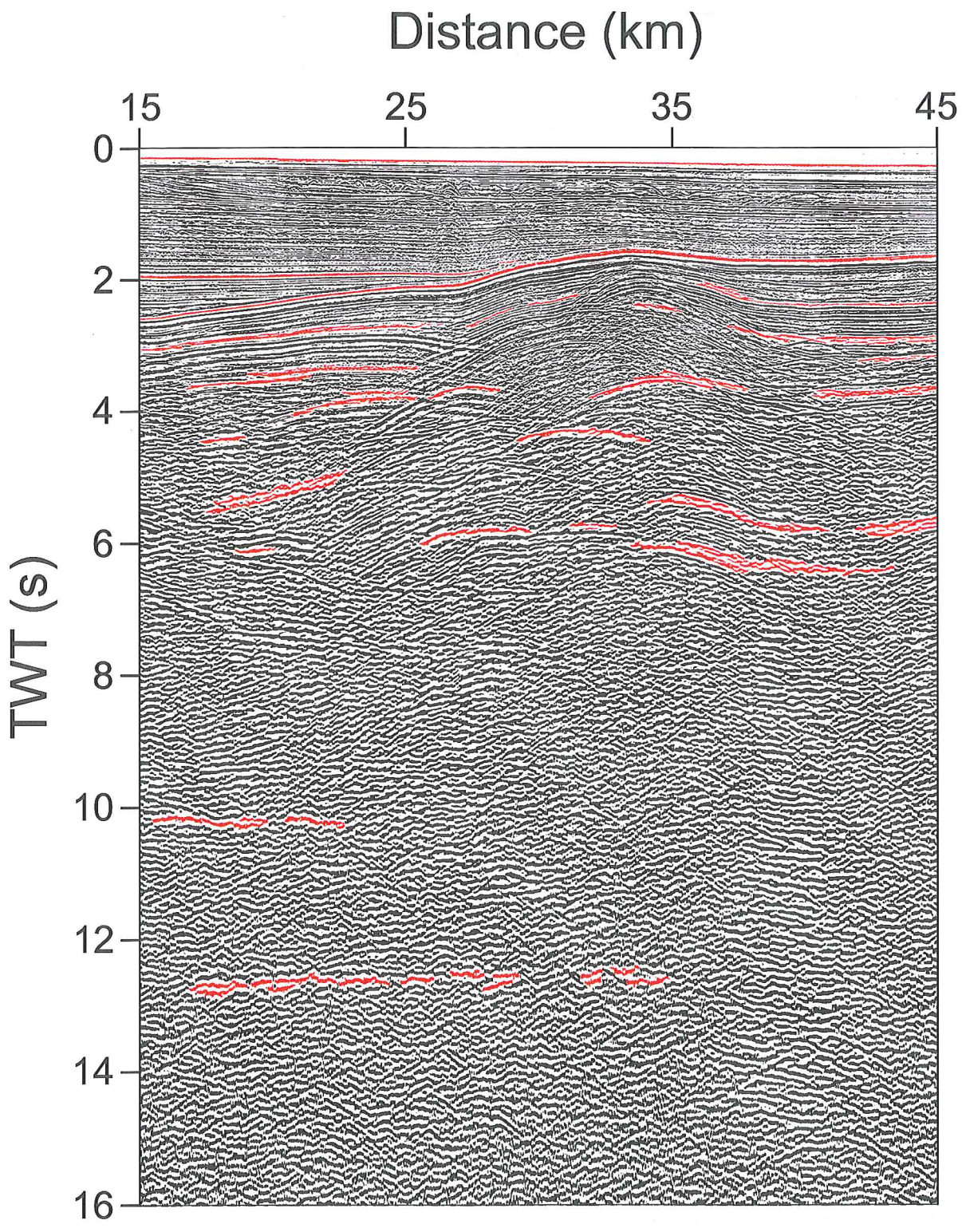

Figure 2: CROP M-15 seismic line (part).

processing sequence to a set of synthetic common-shot profiles computed with the variable-density acoustic wave equation.

The numerical solver consists of the pseudospectral Fourier method for computing the spatial derivatives, and a 2nd-order leap-frog method for time integration (Carcione et al., 1994). An averaging method, developed by Zeng and West (1996), is used to reduce spurious diffractions arising from an inappropriate modelling of curved and dipping interfaces (the so-called staircase effect). It is based on a spatially weighted averaging of the model properties.

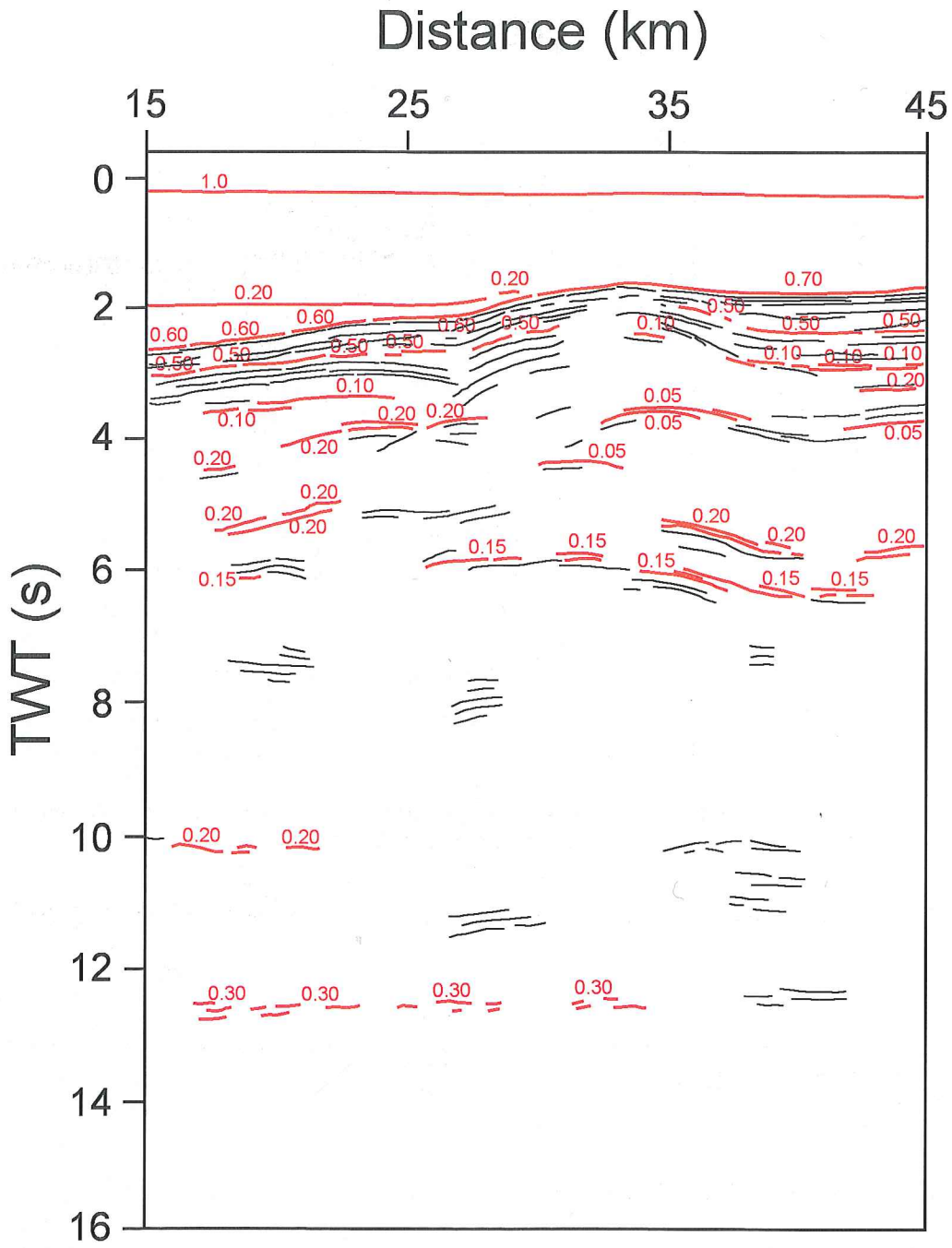

Figure 3: Schematic line drawing of CROP M-15 seismic line. The numbers indicate the relative amplitude of the events highlighted in Figure 2.

2. THE MODELLING TECHNIQUE

The variable-density wave equation for elliptically anisotropic media is

$$\rho c^2 \frac{\partial}{\partial x}\left(\frac{1}{\rho}\frac{\partial p}{\partial x}\right) + \rho c_3^2 \frac{\partial}{\partial z}\left(\frac{1}{\rho}\frac{\partial p}{\partial z}\right) = \frac{\partial^2 p}{\partial t^2} + s, \tag{1}$$

where $p(x, z, t)$ is the pressure field, $\rho(x, z)$ is the material density, $c(x, z)$ is the horizontal P-wave velocity, $c_3(x, z)$ is the vertical P-wave velocity, and $s(x, z, t)$ is the source. Assuming a plane wave kernel

$$\exp\left[\mathrm{i}\omega(t - s_x x - s_z z)\right],$$

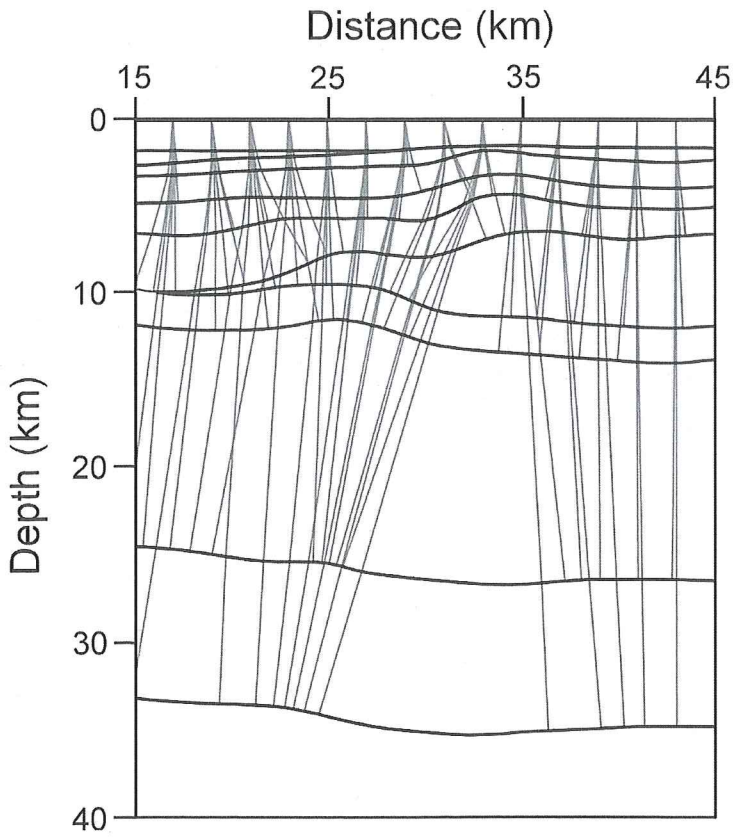

Figure 4: First version of the geological model obtained from zero-offset ray tracing. The zero-offset ray paths are indicated.

where ω is the angular frequency and s_i are the slowness components, we obtain the dispersion relation

$$\frac{s_x^2}{1/c^2} + \frac{s_z^2}{1/c_3^2} = 1. \tag{2}$$

This is an ellipse with semiaxes $1/c$ and $1/c_3$. We assume that the major semiaxis of the ellipse is vertical, that is $c_3 \leqslant c$. Seismic anisotropy is usually reported as a percent,

$$A = 100\left(1 - \frac{c_3}{c}\right) \tag{3}$$

(e.g., Rudnick and Fountain, 1995). The isotropic case is obtained for $c_3 \equiv c$.

We consider the source term

$$s(x, z, t) = \delta(x - x_0)\delta(z - z_0)h(t), \tag{4}$$

where δ is Dirac's delta, (x_0, z_0) is the source location and $h(t)$ is the source time-history (a Ricker-type function in our simulations).

To derive the exploding-reflector isotropic wave equation, with the non-reflecting – constant impedance – condition, we assume that the acoustic impedance

$$I = \rho c \tag{5}$$

is constant throughout the model space. Using this condition, Equation (1) becomes

$$c\frac{\partial}{\partial x}\left(c\frac{\partial p}{\partial x}\right) + c\frac{\partial}{\partial z}\left(c\frac{\partial p}{\partial z}\right) = \frac{\partial^2 p}{\partial t^2} + s \tag{6}$$

(Baysal et al., 1984; Carcione et al., 1994). The normal-incidence reflection coefficient is zero for this equation, and it becomes the constant density wave equation when the velocity is constant. We place a source on each grid

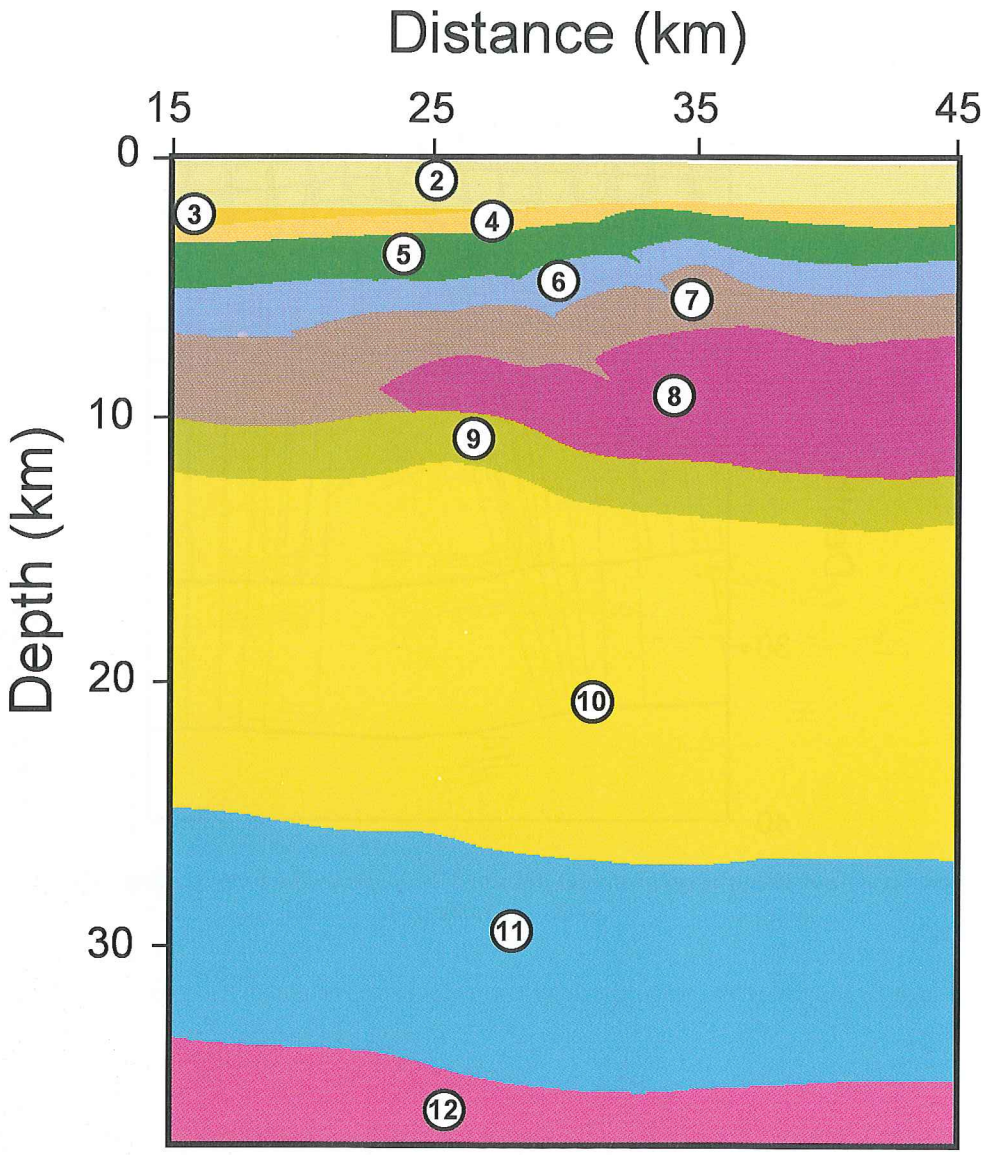

Figure 5: Geological model in terms of seismic velocity and mass density, used for the exploding-reflector simulations. The numbers denote the layers indicated in Table 2.

point (i, j) defining the interfaces,

$$s(x, z, t) = R\delta(x - x_i)\delta(z - z_j)h(t), \tag{7}$$

where R is the normal-incidence reflection coefficient, and (x_i, z_j) is the source location. The normal-incidence reflection coefficient is

$$R = \frac{I_2 - I_1}{I_1 + I_2} \tag{8}$$

(DeSanto, 1992, p. 5), where 1 and 2 denote the upper and lower media.

Because the wave equation is linear, seismograms with different dominant frequencies – and time histories – can be implemented by convolving $h(t)$ with only one simulation obtained with $\delta(t)$ as a source (a discrete delta with strength $1/\mathrm{d}t$).

Scattering due to heterogeneities in the crust and mantle is considered.

Table 2
Acoustic properties. P-wave velocities, anisotropy parameter, density, autocorrelation distance, maximum velocity perturbation and fractal number

Layer	Medium	c (km/s)	A (%)	ρ (g/cm^3)	a (m)	Δc_0 (m/s)	ν
1	Adriatic Sea	1.5	0	1.03	–	–	–
2	Quaternary and Upper Pliocene	2	0	2	–	–	–
3	Lower Pliocene	2.3	0	2.1	–	–	–
4	Miocene to Upper Eocene	3.3	0	2.4	–	–	–
5	Lower Eocene and Cretaceous	5	0	2.5	–	–	–
6	Jurassic	5.4	0	2.55	–	–	–
7	Dolomia Principale	6.3	0	2.55	–	–	–
8	Permo-Triassic Evaporite	6	0	2.7	–	–	–
9	Permian and Pre-Evaporite Triassic	5.5	0	2.5	–	–	–
10	Upper crust	6	3	2.67	200	480	0.15
11	Lower crust	7	5	2.69	150	420	0.2
12	Upper mantle	8	6	3.28	300	640	0.18

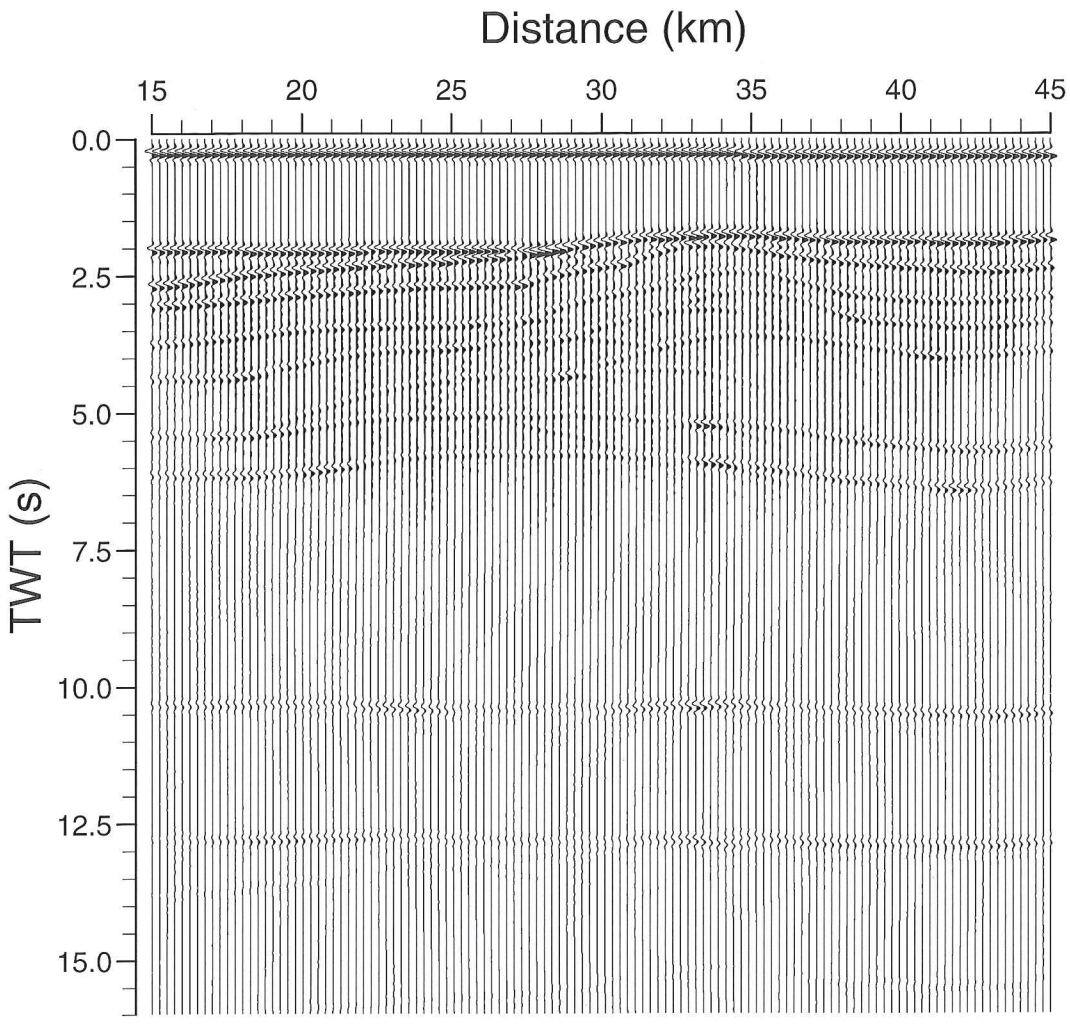

Figure 6: Exploding-reflector response of the model displayed in Figure 5.

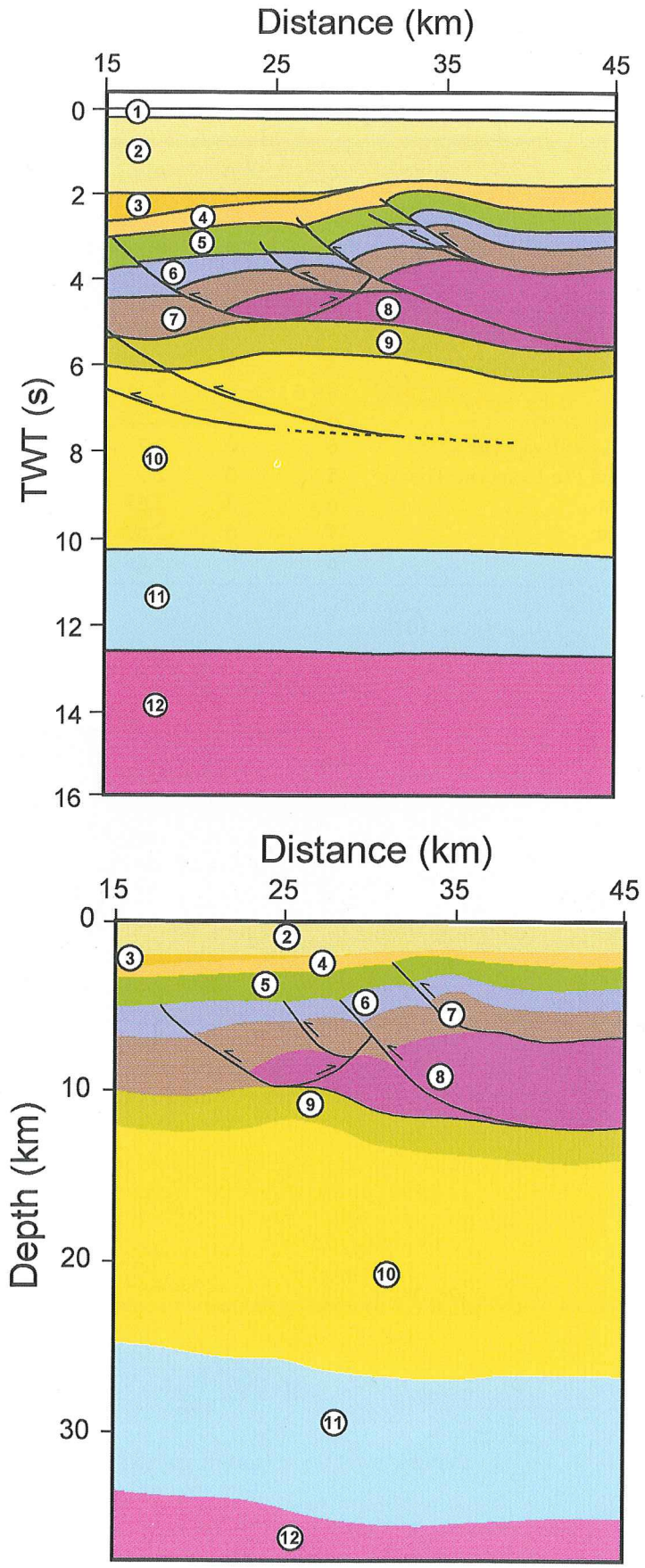

Figure 7: Seismogeological section – in two-way travel time (upper picture) and depth (lower picture) – after a re-interpretation on the basis of the ray-tracing results, the exploding-reflector simulations and a priori geological information.

Let Δc_0 be the maximum deviation of the velocity field from the background value c_0. The velocity field at (x, z) is first subjected to the variations $(\Delta c)^r$, such that

$$-\Delta c_0 \leqslant (\Delta c)^r \leqslant \Delta c_0, \tag{9}$$

where $(\Delta c)^r$ is obtained from a 2-D random generator, and the superindex "r" denotes random. (Random numbers between 0 and 1 are generated and then scaled to the interval $[-1, 1]\Delta c_0$.)

Small-scale P-wave velocity variations in the lithosphere are well described by the von Kármán autocovariance function (Frankel and Clayton, 1986; Holliger, 1997). The corresponding wavenumber-domain power spectrum is

$$C(k_x, k_z) = K(1 + k^2 a^2)^{-(\nu + N/2)}, \tag{10}$$

where $k = \sqrt{k_x^2 + k_z^2}$ is the wavenumber, a is the correlation length, ν $(0 < \nu < 1)$ is a self-similarity coefficient, K is a normalization constant, and N is the Euclidean dimension. The von Kármán correlation function describes self-affine, fractal processes of fractal dimension $N + 1 - \nu$ at a scale smaller than a.

The velocity is then calculated as

$$c(x, z) = c_0 \pm \Delta c(x, z), \tag{11}$$

where

$$\widetilde{\Delta c}(k_x, k_z) = \widetilde{(\Delta c)}^r (k_x, k_z) C(k_x, k_z), \tag{12}$$

with $\widetilde{(\Delta c)}^r (k_x, k_z)$ being the Fourier transform of $(\Delta c)^r (x, z)$. (The tilde denotes the space Fourier transform.)

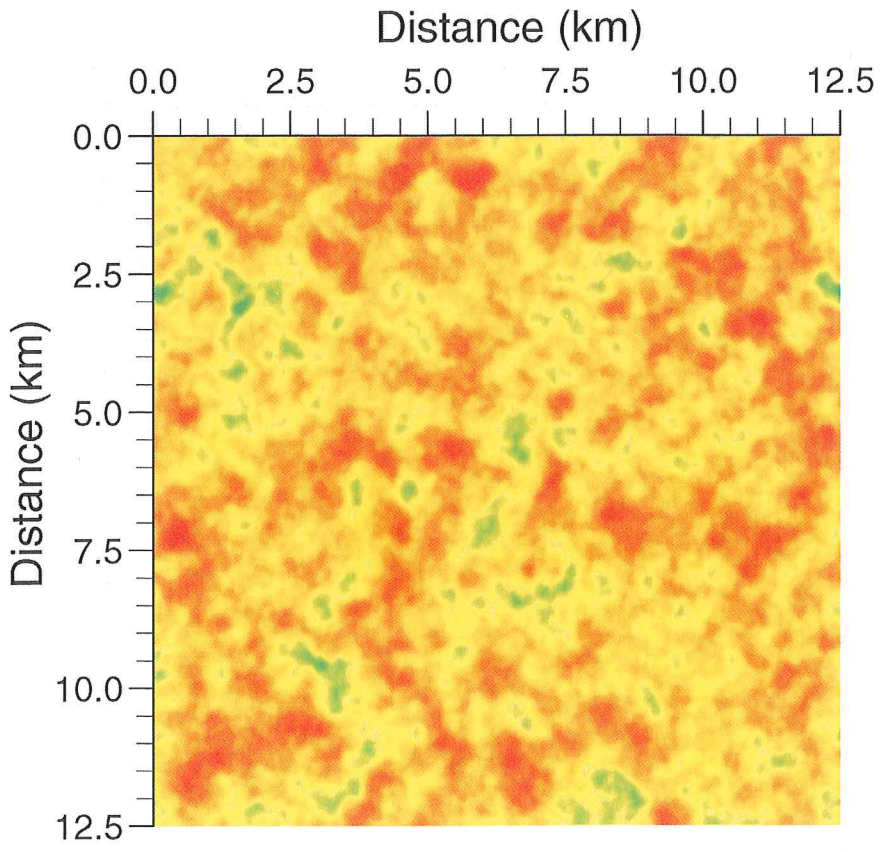

Figure 8: Velocity field perturbations for part of the upper mantle obtained from the von Kármán autocovariance function (see Table 2).

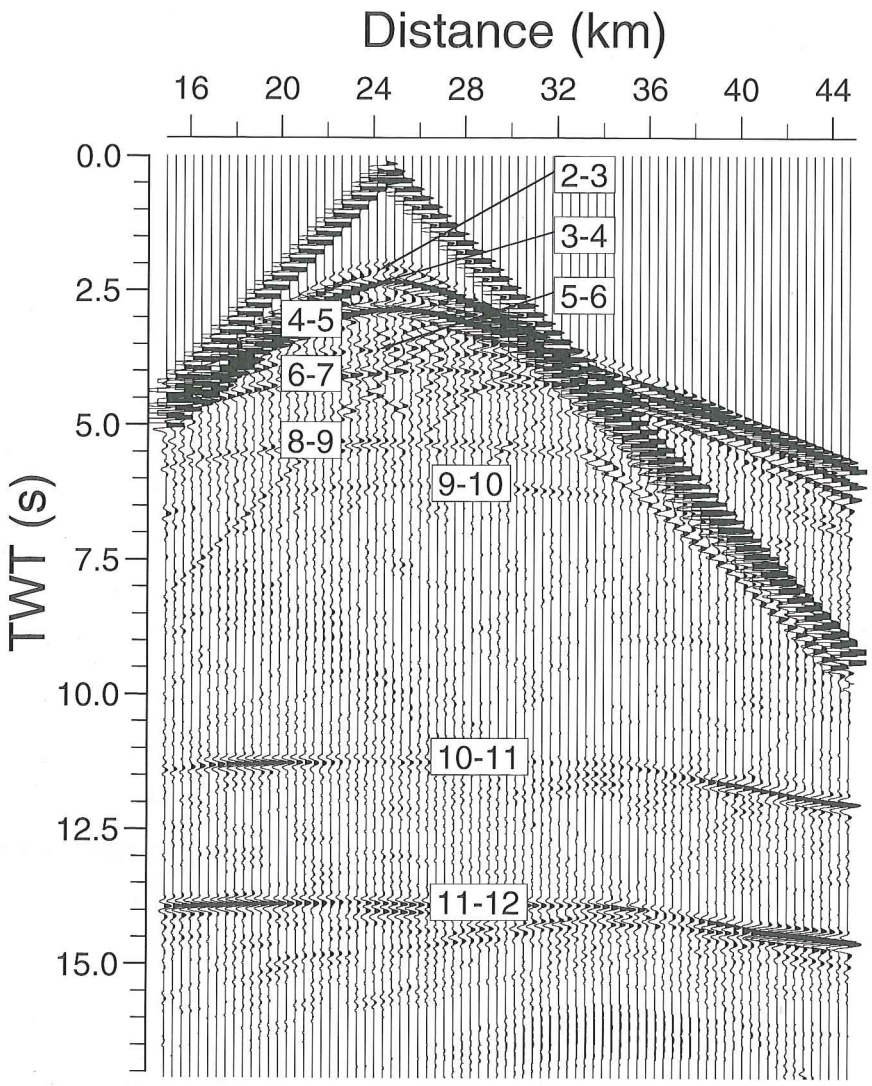

Figure 9: Common-shot gather corresponding to the model shown in Figure 7. The labels denote the reflection events generated at the interfaces indicated in Figure 7.

The spatial derivatives are computed by using the Fourier method. The spectral coefficients are calculated with the fast Fourier transform (FFT) (Fornberg, 1996; Carcione, 2001, p. 303). The time integration of Equations (1) and (6) is performed with a standard second-order differencing scheme (e.g., Celia and Gray, 1992).

3. THE DEEP SEISMIC EXPLORATION SECTION CROP M-15

The location of the CROP M-15 seismic section in the Adriatic Sea is shown in Figure 1. A time section is displayed in Figure 2 (the processing technique is standard). The stronger seismic events are plotted in Figure 3 (line drawing). In general, the numbers indicate the relative amplitudes of the events. In this area, we observe a thick undeformed continental crust, where the sediment column, and upper and lower crust macrointervals can be reliably identified. The section shows the gentle compressive deformation of the frontal Dinaric belt, where the platform slightly thrusts along a high-angle fault over the basinal succession in Oligocene-Miocene times (Finetti and Del Ben, this volume, Chapter 22).

The first phase of the modelling approach is to use a zero-offset ray-tracing algorithm (iteratively) to obtain the location of the geological interfaces. A first estimation of the seismic velocities is obtained from a priori geological and geophysical information for the study area. P-wave seismic-velocity values are based on the data published by Christensen (1989), Rudnick and Fountain (1995) and Brittan and Warner (1996). A first version of the geological model is shown in Figure 4, where the main zero-offset ray trajectories are indicated. Due to the limitations of the ray-tracing algorithm, structures such as faults planes cannot be simulated.

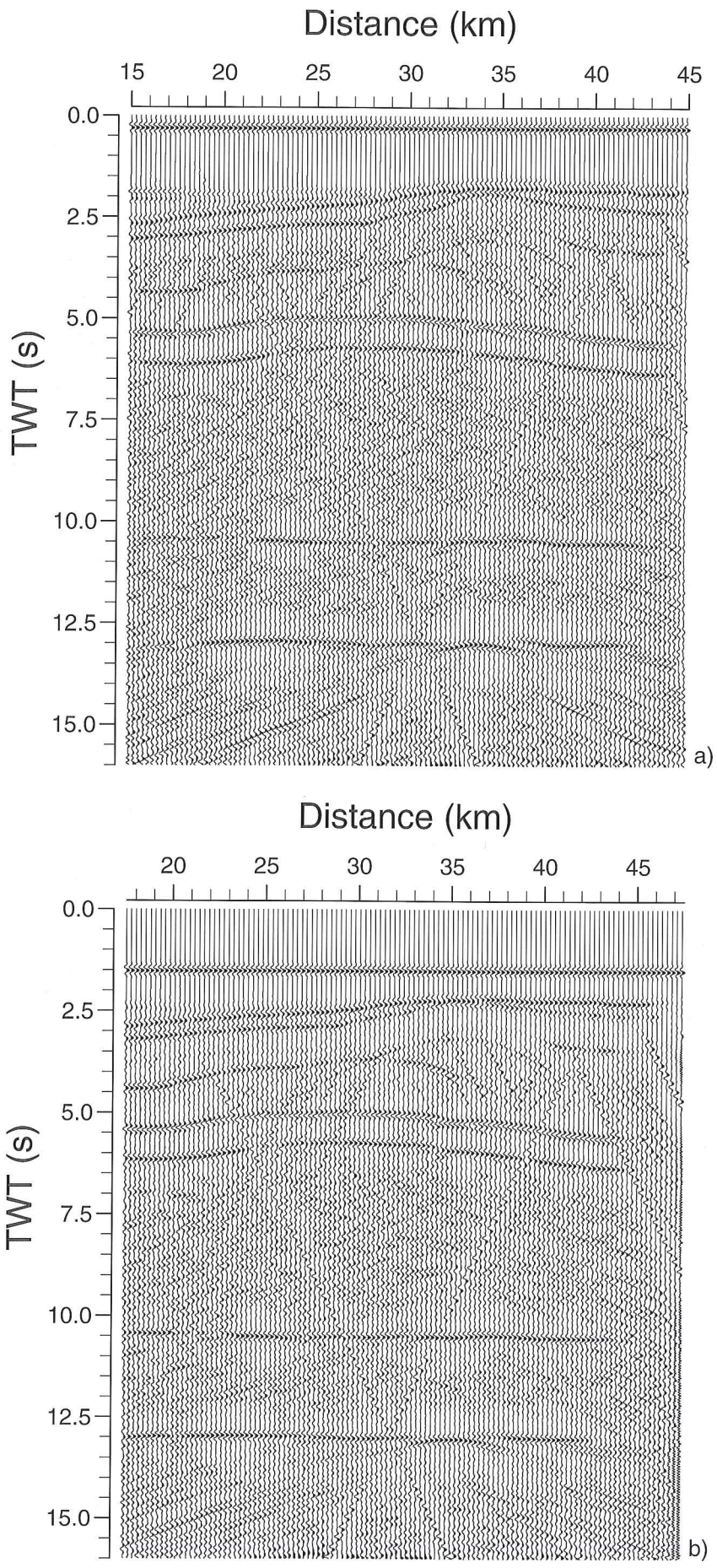

Figure 10: Near-offset section (a) and far-offset section (b) corresponding to the model shown in Figure 7.

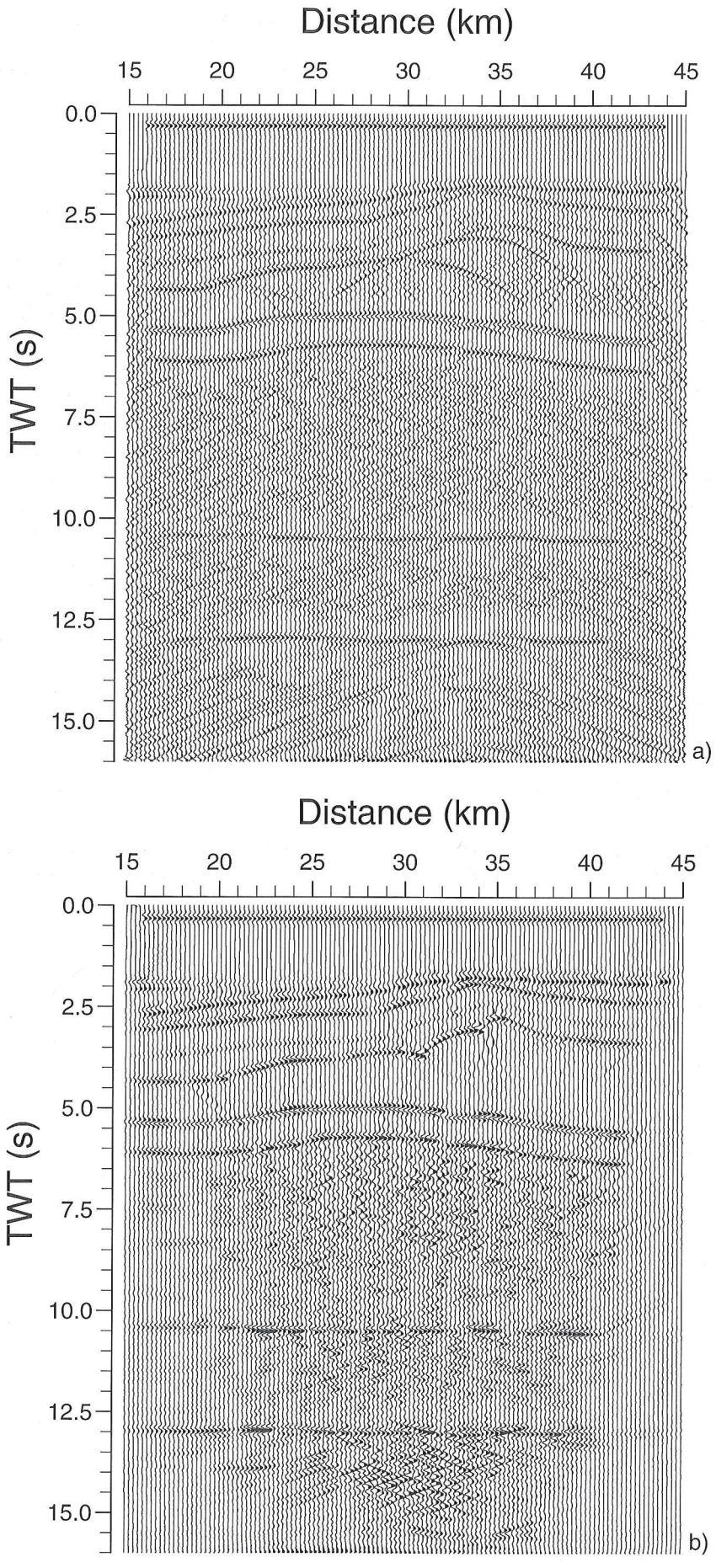

Figure 11: Stacked section (a) and time-migrated section (b) corresponding to the model shown in Figure 7.

The model is refined by using exploding-reflector simulations. In the exploding-reflector algorithm the source strength is proportional to the reflection coefficient, which is proportional to the acoustic-impedance contrast. Thus, the density of each layer is obtained from data provided by Rudnick and Fountain (1995), and using the relative amplitudes indicated in Figure 3. The mesh has 1080×1200 points, with a grid spacing of 31 m. In order to avoid wraparound, absorbing strips of length 60 grid points are implemented at the boundaries of the numerical mesh. The dominant frequency of the source is 6 Hz, and the wavefield is computed by using a time step of 1 ms. The final geological model (see Figure 5 and Table 2) is obtained after computing many exploding-reflector sections and comparing the simulations with the real stacked section (anisotropy and scattering effects are not taken into account in this phase). Figure 6 shows the exploding-reflector seismic section. The improvement over the model shown in Figure 4 consists in the inclusion of fault planes based on the presence of diffraction events. The interpreter plays an important role in this phase, integrating a priori knowledge of the regional tectonic features. Figure 7 shows the geological section in two-way travel time (a) and depth (b), after a re-interpretation on the basis of the preceding information and a priori regional geological information.

In the following, we consider anisotropy and scattering effects according to the values given in Table 2. Since the wavefront is elliptical, the moveout velocity is the velocity for a wave traveling in the horizontal direction. This velocity, c, is obtained from surface measurements (Levin, 1978). Figure 8 shows the perturbation of the velocity field ($\Delta c(x, z)$) of a representative part of the upper mantle. In order to simulate ten-fold CMP acquisition, 120 common shots with 80 split-symmetric channels are computed. The shot interval is 248 m, and the group spacing is 62 m. The mesh has 600×720 points, a grid spacing of 62 m, and 60 grid points for each absorbing strip. The positions of the first and last shots are $x = 15$, and $x = 44.76$ km, respectively. Figure 9 shows a common-shot gather, where the indices denote the reflection events generated at the different interfaces indicated in Figures 5 and 7. Figure 10 shows two common-offset sections, corresponding to the near offsets (a) and far offsets (b). They resemble the stacked section, in particular the near-offset section. The stacked section and its post-stack time migration are displayed in Figures 11(a) and 11(b), respectively. The strength of the events in the unmigrated section agree fairly well with the values indicated in Figure 2, and the migrated section is in good agreement with the model shown in Figure 7.

4. CONCLUSIONS

The procedure used to simulate the CROP M-15 seismic line involves: (i) line drawing, to identify the location and strength of the main events; (ii) ray tracing, to generate a first version of the geological model in terms of seismic velocities; (iii) exploding-reflector experiments, to generate a geological model in terms of seismic velocity and mass density; (iv) refining of the model by the interpreter on the basis of a priori geological and geophysical information (inclusions of fault planes, etc.).

The model is further improved by considering random heterogeneities, which characterize the seismic response of the crust and mantle at different scales. The result is a complete characterization of the geological setting, with the possibility of calculating realistic common-shot seismograms to further investigate and improve the interpretation of the different geological structures.

It is important to point out that the modelling phase is a validating tool of the interpretation process. A substantial role is played by the ability and knowledge of the interpreter, who integrates a priori knowledge of the main tectonic characteristics of the area under study.

ACKNOWLEDGEMENTS

This work was funded in part by MURST (Ministry of University, Scientific Research and Technology) under the framework of COFIN-2000 granted to I.R. Finetti.

REFERENCES

Baysal, E., Kosloff, D.D., Sherwood, J.W.C., 1984. A two-way nonreflecting wave equation. Geophysics 49, 132–141.

Brittan, J., Warner, M., 1996. Seismic velocity, heterogeneity, and the composition of the lower crust. Tectonophysics 264, 249–259.

Carcione, J.M., 2001. Wave Fields in Real Media. Wave Propagation in Anisotropic, Anelastic and Porous Media. In: Handbook of Geophysical Exploration, vol. 31. Pergamon Press.

Carcione, J.M., Böhm, G., Marchetti, A., 1994. Simulation of a CMP seismic section. J. Seis. Expl. 3, 381–396.

Celia, M.A., Gray, W.G., 1992. Numerical Methods for Differential Equations. Fundamental Concepts for Scientific and Engineering Applications. Prentice-Hall.

Christensen, N.I., 1989. Reflectivity and seismic properties of the deep continental crust. J. Geophys. Res. 94 (B12), 17793–17804.

DeSanto, J.A., 1992. Scalar Wave Theory. Springer Series on Wave Phenomena. Springer-Verlag, Berlin.

Fagin, S.W., 1992. Seismic Modeling of Geological Structures: Applications to Exploration Problems. Geophysical Development Series, vol. 2. Society of Exploration Geophysicists.

Finetti, I. (Ed.), 1994. CROP project, offshore crustal seismic profiling in the central Mediterranean. Boll. Geof. Teor. Appl. 36 (1994) 1–536.

Finetti, I.R., Boccaletti, M., Bonini, M., Del Ben, A., Geletti, R., Pipan, M., Sani, F., 2001. Crustal section based on CROP seismic data across the North Tyrrhenian–Northern Apennines–Adriatic Sea. Tectonophysics 343, 135–163.

Finetti, I.R., Del Ben, A., this volume. Crustal tectono-stratigraphic setting of the Adriatic sea from new CROP seismic data. Chapter 22.

Fornberg, B., 1996. A Practical Guide to Pseudospectral Methods. Cambridge University Press.

Frankel, A., Clayton, R.W., 1986. Finite difference simulations of seismic scattering: implications for the propagation of short-period seismic waves in the crust and models of crustal heterogeneity. J. Geophys. Res. 91 (B6), 6465–6489.

Guest, W.S., Thomson, C.J., 1992. A source of significant transverse isotropy arrivals from an isotropic–anisotropic interface, e.g., the Moho. Geophys. J. Internat. 111, 309–318.

Holliger, K., 1997. Seismic scattering in the upper crystalline crust based on evidence from sonic logs. Geophys. J. Internat. 128, 65–72.

Levin, F., 1978. The reflection, refraction, and diffraction of waves in media with an elliptical velocity dependence. Geophysics 43, 528–537.

Mazzotti, A.P., Stucchi, E., Fradelizio, G.L., Zanzi, L., Scandone, P., 2000. Seismic exploration in complex terrains: a processing experience in the Southern Apennines. Geophysics 65, 1402–1417.

Morgante, A., Barchi, M.R., D'Offizi, S., Minelli, G., Pialli, G., 1998. The contribution of seismic modeling to the interpretation of the CROP-03 line. Mem. Soc. Geol. It. 52, 91–100.

Priolo, E., 1999. 2-D spectral element simulation of destructive ground shaking in Catania (Italy). J. Seismology 3, 289–309.

Rabbel, W., Gajewski, D. (Eds.), 1999. Seismic exploration of the deep continental crust. Pure Appl. Geophys. 156 (1999) 1–370.

Rudnick, R.L., Fountain, D.M., 1995. Nature and composition of the continental crust: a lower crustal perspective. Rev. Geophys. 33 (3), 267–309.

Yarnold, J.C., Johnson, R.A., Sorensen, L.S., 1993. Identification of multiple generations of crosscutting "domino"-style faults: insights from seismic modeling. Tectonics 12, 159–168.

Zeng, X., West, G.F., 1996. Reducing spurious diffractions in elastic wavefield calculations. Geophysics 61, 1436–1439.